

Evolving Metric Learning for Incremental and Decremental Features

Jiahua Dong, Yang Cong, *Senior Member, IEEE*, Gan Sun, Tao Zhang and Xiaowei Xu

Abstract—Online metric learning has been widely exploited for large-scale data classification due to the low computational cost. However, amongst online practical scenarios where the features are evolving (*e.g.*, some features are vanished and some new features are augmented), most metric learning models cannot be successfully applied into these scenarios although they can tackle the evolving instances efficiently. To address the challenge, we propose a new online Evolving Metric Learning (EML) model for incremental and decremental features, which can handle the instance and feature evolutions simultaneously by incorporating with a smoothed Wasserstein metric distance. Specifically, our model contains two essential stages: the Transforming stage (T-stage) and the Inheriting stage (I-stage). For the T-stage, we propose to extract important information from vanished features while neglecting non-informative knowledge, and forward it into survived features by transforming them into a low-rank discriminative metric space. It further explores the intrinsic low-rank structure of heterogeneous samples to reduce the computation and memory burden especially for highly-dimensional large-scale data. For the I-stage, we inherit the metric performance of survived features from the T-stage and then expand to include the augmented new features. Moreover, the smoothed Wasserstein distance is utilized to characterize the similarity relations among the complex and heterogeneous data, since the evolving features in the different stages are not strictly aligned. In addition to tackling the challenges in one-shot case, we also extend our model into multi-shot scenario. After deriving an efficient optimization method for both T-stage and I-stage, extensive experiments on several benchmark datasets verify the superiority of our model.

Index Terms—Online metric learning, instance and feature evolutions, smoothed Wasserstein distance, low-rank constraint.

I. INTRODUCTION

Metric learning has been successfully extended into many fields, *e.g.*, face identification [1], object recognition [2] and medical diagnosis [3]. To efficiently solve the large-scale streaming data problem, learning a discriminative metric in an online manner (*i.e.*, online metric learning [4],

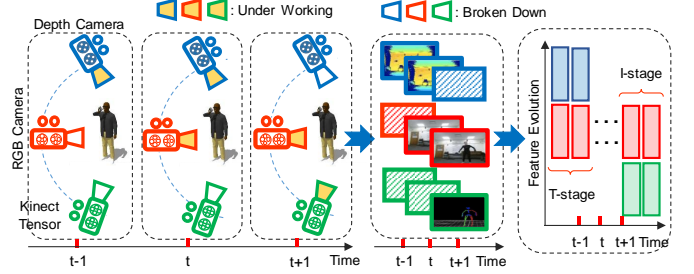


Fig. 1. Illustration example of feature evolution on human motion recognition task, where the blue, red and green colors respectively indicate different kinds of features collected from depth, RGB and kinect sensors with different lifespans. The features collected from different sensors are incremental in the T-stage, and decremental in the I-stage.

[5]) attracts lots of appealing attentions. Generally, most online metric learning models pay attention to the fast metric updating strategies [6]–[9] or fast similarity searching methods [5], [8], [10] for large-scale streaming data.

However, these existing online metric learning methods [11], [12] only focus on instance evolution, and ignore the feature evolution in many real applications where some features are vanished and some new features are augmented. Take the human motion recognition [13] as an example (*i.e.*, Fig. 1), the emerging of new kinect sensor and the sudden damage of depth camera will respectively lead to a corresponding increase and decrease in the feature dimensionality of the input data, which heavily cripples the performance of the pre-trained model [13]. Another interesting example is that different kinds of sensors (*e.g.*, radioisotope, trace metal and biological sensors [14]) are deployed for the research of dynamic environment monitoring in full aspects, some sensors (features) expire whereas some new sensors (features) are deployed when different electrochemical conditions and lifespans occur. A fixed or static online metric learning model will fail to make full use of sensors (features) evolved in this way. Therefore, how to establish a novel metric learning model to simultaneously handle instance evolution, and incremental and decremental features amongst these online practical systems is our focus in this paper.

To address the challenges above, as shown in Fig. 2, we present a new online Evolving Metric Learning (EML) model for incremental and decremental features, which can exploit streaming data with both instance and feature evolutions in an online manner. To be specific, the proposed EML model consists of two significant stages, *i.e.*, the Transforming stage (T-stage) and the Inheriting stage (I-stage). 1) In the T-stage where features are decremental, we propose to explore

This work is supported by Ministry of Science and Technology of the Peoples Republic of China (2019YFB1310300) and National Nature Science Foundation of China under Grant (61722311, U1613214, 61821005, 61533015). (*Corresponding author: Yang Cong.*)

J. Dong and T. Zhang are with the State Key Laboratory of Robotics, Shenyang Institute of Automation, Chinese Academy of Sciences, Shenyang 110016, China, and also with Institutes for Robotics and Intelligent Manufacturing, Chinese Academy of Sciences, Shenyang 110016, China, and also with University of Chinese Academy of Sciences, Beijing 100049, China (e-mail: dongjiahua@sia.cn, zhangtao2@sia.cn).

Y. Cong and G. Sun are with the State Key Laboratory of Robotics, Shenyang Institute of Automation, Chinese Academy of Sciences, Shenyang 110016, China, and also with Institutes for Robotics and Intelligent Manufacturing, Chinese Academy of Sciences, Shenyang 110016, China (e-mail: congyang81@gmail.com, sungan1412@gmail.com).

X. Xu is with Department of Information Science, University of Arkansas at Little Rock, Arkansas 72204, USA (e-mail: xwxu@ualr.edu).

the important information and data structure from vanished features, and transform them into a low-rank discriminative metric space of survived features, which can be used to assist the learning of following metric tasks. Moreover, it explores the intrinsic low-rank structure of the streaming data, which efficiently reduces the computation and memory costs especially for highly-dimensional large-scale samples. 2) For the I-stage where features are incremental, based on the learned discriminative metric space in the T-stage, we inherit the metric performance of survived features from T-stage and then expand to include new augmented features. Furthermore, to better explore the similarity relations amongst the heterogeneous data, a smoothed Wasserstein distance is applied into both T-stage and I-stage where the evolving features in different stages are strictly unaligned and heterogeneous. For the model optimization, we derive an efficient optimization method to solve both T-stage and I-stage. Besides, our model can be successfully extended from one-shot scenario into multi-shot scenario. Comprehensive experimental results on several benchmark datasets can strongly support the effectiveness of our proposed EML model.

The main contributions of this paper are summarized as follows:

- We propose an online Evolving Metric Learning (EML) model for incremental and decremental features to tackle both instance and feature evolutions simultaneously. To our best knowledge, this is the first attempt to tackle this crucial, but rarely-researched challenge in the metric learning field.
- We present two stages for both feature and instance evolutions, *i.e.*, the Transforming stage (T-stage) and the Inheriting stage (I-stage), which can not only make full use of the vanished features in the T-stage, but also take advantage of streaming data with new augmented features in the I-stage.
- A smoothed Wasserstein distance is incorporated into metric learning to characterize the similarity relations for heterogeneous evolving features in different stages. After deriving an alternating direction optimization algorithm to optimize our EML model, extensive experiments on benchmark datasets validate the effectiveness of our proposed model.

II. RELATED WORK

This section first provides a brief overview about online metric learning for instance evolution. Then some representative works about feature evolution are introduced.

A. Online Metric Learning

Online metric learning has been widely explored for instance evolution to learn large-scale streaming data, which can mainly be divided into two categories: Mahalanobis distance-based and bilinear similarity-based methods. For the Mahalanobis distance-based methods, POLA [15] is the first attempt to learn the optimal metric in an online way. Then several variants [5], [10], [16] extend this idea by the fast similarity searching strategies, *e.g.*, [8] propose a regularized

online metric learning model with the provable regret bound. Besides, pairwise constraint [8] and triplet constraint [9] are adopted to learn a discriminative metric function. Generally, triplet constraints are more effective than pairwise constraints to learn a discriminative metric function [9], [17]. For the bilinear similarity-based models, OASIS [4] is proposed to learn a similarity metric for image similarity, and SOML [18] aims to learn a diagonal matrix for high dimensional cases with the similar setting as OASIS. Besides, [19] presents an Online Multiple Kernel Similarity to tackle multi-modal tasks. However, these recently-proposed Mahalanobis distance-based and bilinear similarity-based methods cannot exploit the discriminative similarity relations for the strictly unaligned heterogeneous data in different evolution stages.

B. Feature Evolution

For the feature evolution, with the assumption that there exists samples from both vanished feature space and augmented feature space in an overlapping period, [20] develops a evolvable feature streaming learning model by reconstructing the vanished features and exploiting it along with new emerging features for large-scale streaming data. [21] proposes an one-pass incremental and decremental learning model for streaming data, which consists of compressing stage and expanding stage. Different from [20], [21] assumes that there are overlapping features instead of overlapping period. Similarly with [21], [22] focuses on learning the mapping function from two different feature spaces by using optimal transport technique. [23], [24] intend to deal with trapezoidal data stream where both instance and feature can doubly increase. However, the new emerging data always have overlapping features with the previously existing data. [25] develops a feature incremental random forest model to improve performance for a small amount of data with newly incremental features, which enables the model generalize well to the emergence of incremental features.

Amongst the discussion above, there are no any feature evolution models highly related to our work except for OPID (OPIDe) [21]. However, there are several key differences between [21] and our EML model: 1) Our work is the first attempt to explore both instance and feature evolutions simultaneously via T-stage and I-stage in the metric learning field, when compared with [21]. 2) Due to the strictly unaligned evolving features in the different stages, we utilize the smoothed Wasserstein distance to characterize the similarity relations among the complex and heterogeneous data, rather than the Euclidean distance in [21]. 3) Compared with [21], the low-rank regularizer for distance matrix could efficiently learn a discriminative low-rank metric space, while neglecting non-informative knowledge for heterogeneous data in different feature evolution stages.

III. EVOLVING METRIC LEARNING (EML)

In this section, we first review online metric learning, and then detailedly introduce how to tackle both instance and feature evolutions via our proposed EML model.

A. Revisit Online Metric Learning

Metric learning aims to learn an optimal distance measure matrix according to the different measure functions, *e.g.*, Mahalanobis distance function: $d_M(x_p, x_q) = \sqrt{(x_p - x_q)^\top M (x_p - x_q)}$, where $x_p \in \mathbb{R}^d$ and $x_q \in \mathbb{R}^d$ are the p -th and q -th samples, respectively. $M \in \mathbb{R}^{d \times d}$ is the symmetric positive semi-definite matrix, which can be decomposed as $L^\top L$ [5], where $L \in \mathbb{R}^{r \times d}$ (r is the rank of M) is the transformation matrix. Then the Mahalanobis distance function between x_p and x_q can be rewritten as $d_L(x_p, x_q) = \|L(x_p - x_q)\|_2^2$. Given an online constructed triplet (x_p, x_q, x_k) , L could be updated in an online manner via the Passive-Aggressive algorithm [26], *i.e.*,

$$L_t = \arg \min_L \frac{1}{2} \|L - L_{t-1}\|_F^2 + \frac{\gamma}{2} \ell_L(x_p, x_q, x_k), \quad (1)$$

where $\ell_L(x_p, x_q, x_k) = [1 + d_L(x_p, x_q) - d_L(x_p, x_k)]_+$ is a hinge loss function. $[z]_+$ represents $\max(0, z)$, x_p and x_q belong to the same class, and x_p and x_k belong to the different classes. $\gamma \geq 0$ is the regularization parameter.

However, most existing online metric learning models (*e.g.*, Eq. (1)) only focus on instance evolution with a fixed feature dimensionality, which is unable to be used in the feature evolution scenario, *i.e.*, streaming data with incremental and decremental features. Furthermore, the learned distance matrix L of Eq. (1) is not discriminative enough to explore similarity relations of the complex and heterogeneous samples, whose evolving features in different evolution stages are not strictly aligned [27].

B. The Proposed EML Model

In this subsection, we first present the introductions of integrating a smoothed Wasserstein distance into online metric learning formulation (*i.e.*, Eq. (1)) to characterize the similarity relations of heterogeneous data with feature evolution in the different stages. Then the details about how to tackle feature evolution via T-stage and I-stage in one-shot scenario are elaborated, followed by the extension of multi-shot case.

1) *Online Wasserstein Metric Learning*: Wasserstein distance [28] is an optimal transportation to move all the earth from the source to the destination, which requires the minimum amount of efforts. Formally, given two signatures $P = \{(x_{pi}, \mu_{pi})\}_{i=1}^m$ and $Q = \{(x_{qj}, \mu_{qj})\}_{j=1}^n$, the smoothed Wasserstein distance [29] between P and Q is:

$$W_\sigma(P, Q) = \min_{F \in \mathbb{F}(P, Q)} \langle D(P, Q), F \rangle - \sigma h(F), \quad (2)$$

$$s.t. \mathbb{F}(P, Q) = \{F | F \mathbf{1}_n = \mu_p, F^\top \mathbf{1}_m = \mu_q, F \geq 0\},$$

where $D(P, Q) = \{d_L(i, j)\}_{i,j=1}^{m,n} \in \mathbb{R}^{m \times n}$ is a distance matrix, and each $d_L(i, j)$ denotes the cost of moving one unit of earth from the source sample x_{pi} to the target sample x_{qj} . $F = \{f(i, j)\}_{i,j=1}^{m,n}$ is the flow network matrix, and each $f(i, j)$ represents the amount of earth moved from x_{pi} to x_{qj} . $\mu_p = \{\mu_{pi}\}_{i=1}^m \in \mathbb{R}^m$ and $\mu_q = \{\mu_{qj}\}_{j=1}^n \in \mathbb{R}^n$ are normalized marginal probability mass vectors. $\sigma \geq 0$ is a balance parameter, and $h(F) = -\langle F, \log(F) \rangle$ is the strictly concave entropic function.

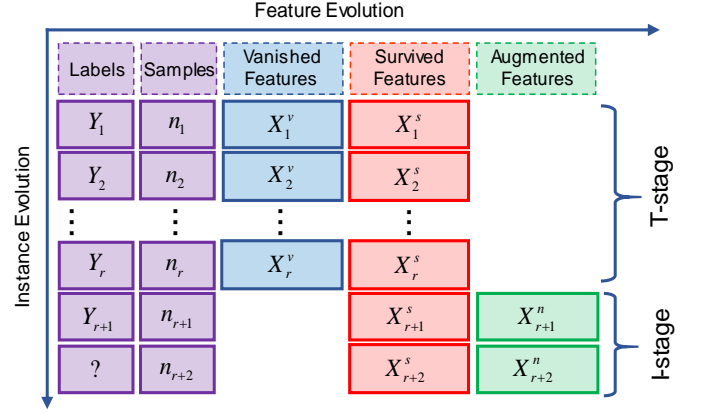


Fig. 2. The illustration of our EML model in one-shot scenario, which evolves features and instances simultaneously via T-stage and I-stage. Different colors denote different kinds of features, *e.g.*, blue, red and green colors denote the vanished, survived and augmented features, respectively. The purple color indicates labels and the number of corresponding samples.

In the Eq. (2), the Mahalanobis distance is employed as ground distance to construct smoothed Wasserstein distance. Thus, each element $d_L(i, j)$ of $D(P, Q)$ in Eq. (2) represents the squared Mahalanobis distance between the source sample x_{pi} of P and the target sample x_{qj} of Q , *i.e.*, $d_L(i, j) = \|L(x_{pi} - x_{qj})\|_2^2$. Given the online constructed triplet (P, Q, K) via [30], where the samples of P and Q belong to the same class, and the samples of P and K belong to different classes. After substituting Mahalanobis distance in Eq. (1) with the smooth Wasserstein distance defined in Eq. (2), online Wasserstein metric learning can be:

$$\min_{L, F} \mathcal{L}_L(P, Q, K) = \frac{1}{2} \|L - L_{t-1}\|_F^2 + \frac{\gamma}{2} \ell_L(P, Q, K), \quad (3)$$

where $\ell_L(P, Q, K) = [1 + W_\sigma(P, Q) - W_\sigma(P, K)]_+$. When compared with the triplet (x_p, x_q, x_k) , each signature in (P, Q, K) consists of several samples belonging to the same class rather than only one sample.

2) *Transforming Stage & Inheriting Stage*: Two essential stages (*i.e.*, T-stage and I-stage) of our proposed EML model for steaming data with feature evolution are elaborated below.

I. Transforming Stage (T-stage): As shown in Fig. 2, suppose that $\{X_i, Y_i\}_{i=1}^r$ denotes the data stream in the T-stage, where $X_i = [X_i^v, X_i^s] \in \mathbb{R}^{n_i \times (d_v + d_s)}$ and $Y_i \in \mathbb{R}^{n_i}$ denote the samples and labels in the i -th batch, respectively. r is the total batches in T-stage and n_i is the number of samples in the i -th batch. Obviously, each instance of X_i contains two kinds of features, *i.e.*, vanished and survived features, and d_v and d_s indicate the corresponding dimensions of vanished features $X_i^v \in \mathbb{R}^{n_i \times d_v}$ and survived features $X_i^s \in \mathbb{R}^{n_i \times d_s}$.

If we directly combine both vanished and survived features to learn a unified metric function, it cannot be used in I-stage where some features are vanished and some other features are augmented. We thus propose to extract important information from vanished features and forward it into survived features by transforming them into a common discriminative metric space. In other words, we want to train a model using only survived features to represent the important information of both vanished and survived features.

In the i -th batch of T-stage, inspired by [30], the triplet (P_i^s, Q_i^s, K_i^s) for survived features is constructed in an online manner, where the samples of $P_i^s \in \mathbb{R}^{n_p \times d_s}$ and $Q_i^s \in \mathbb{R}^{n_q \times d_s}$ belong to the same class while the samples of P_i^s and $K_i^s \in \mathbb{R}^{n_k \times d_s}$ belong to different classes. n_p, n_q and n_k are the numbers of samples in each signature. Similarly, we can construct the triplet (P_i^a, Q_i^a, K_i^a) for all features (including both vanished and survived features), where the samples of $P_i^a \in \mathbb{R}^{n_p \times (d_v + d_s)}$ and $Q_i^a \in \mathbb{R}^{n_q \times (d_v + d_s)}$ belong to same class while the samples of P_i^a and $K_i^a \in \mathbb{R}^{n_k \times (d_v + d_s)}$ belong to different classes.

Let $L^s \in \mathbb{R}^{k \times d_s}$ and $L^a \in \mathbb{R}^{k \times (d_v + d_s)}$ denote the distance matrices trained on survived features and all features in T-stage. Since the dimensions of L^s and L^a are different, it is reasonable to add some essential consistency constraints on the optimal distance matrices L^s and L^a to extract important information from vanished features, and forward it into survived features. Generally, based on the smoothed Wasserstein metric learning in Eq. (3), the formulation of the i -th batch for the T-stage can be expressed as follows:

$$\min_{L^s, L^a, F} \mathcal{L}_{L^s}(P_i^s, Q_i^s, K_i^s) + \mathcal{L}_{L^a}(P_i^a, Q_i^a, K_i^a) + \rho \mathcal{C}_{L^s, L^a}(P_i^s, Q_i^s, K_i^s; P_i^a, Q_i^a, K_i^a) + \lambda \text{rank}(L^s, L^a), \quad (4)$$

where $\mathcal{L}_{L^s}(P_i^s, Q_i^s, K_i^s)$ and $\mathcal{L}_{L^a}(P_i^a, Q_i^a, K_i^a)$ denote the triplet losses of smoothed Wasserstein metric learning on survived features and all features, respectively. $\text{rank}(\cdot) = \text{rank}(L^s) + \text{rank}(L^a)$ denotes the regularization term, which explores the intrinsic low-rank structure of heterogeneous samples. $\rho \geq 0$ and $\lambda \geq 0$ are balance parameters. $\mathcal{C}_{L^s, L^a}(\cdot; \cdot)$ in Eq. (4) is designed to enable the consistence constraint for L^s and L^a , which aims to use only survived features to represent the important information of both vanished and survived features.

Specifically, $\mathcal{C}_{L^s, L^a}(\cdot; \cdot)$ constructs an essential triplet loss of smoothed Wasserstein metric learning on different feature spaces, *i.e.*, all features and survived features. We attempt to compute the smoothed Wasserstein distance between different heterogeneous distributions from vanished features and all features. For example, $W_\sigma(P_i^a, Q_i^s) = \{d_L(u, v)\}_{u,v=1}^{n_p, n_q} \in \mathbb{R}^{n_p \times n_q}$ denotes the smoothed Wasserstein distance between P_i^a from all features and Q_i^s from survived features, where $d_L(u, v) = \|L^a x_{pu}^a - L^s x_{qv}^s\|_2^2$ indicates the Mahalanobis distance between the u -th source sample x_{pu}^a of P_i^a and the v -th target sample x_{qv}^s of Q_i^s . Likewise, $W_\sigma(P_i^a, K_i^s)$, $W_\sigma(P_i^s, Q_i^a)$ and $W_\sigma(P_i^s, K_i^a)$ have similar definitions with $W_\sigma(P_i^a, Q_i^s)$. Formally, the consistence constraint $\mathcal{C}_{L^s, L^a}(\cdot; \cdot)$ is expressed as:

$$\mathcal{C}_{L^s, L^a}(\cdot; \cdot) = [W_\sigma(P_i^a, Q_i^s) - W_\sigma(P_i^a, K_i^s) + 1]_+ + [W_\sigma(P_i^s, Q_i^a) - W_\sigma(P_i^s, K_i^a) + 1]_+. \quad (5)$$

II. Inheriting Stage (I-stage): Suppose $\{X_{r+1}, Y_{r+1}\}$ are the data in the $r+1$ -th batch of I-stage, where $X_{r+1} = [X_{r+1}^s, X_{r+1}^n] \in \mathbb{R}^{n_{r+1} \times (d_s + d_n)}$ indicates the samples and $Y_{r+1} \in \mathbb{R}^{n_{r+1}}$ is the corresponding labels, as shown in Fig. 2. X_{r+1}^s and X_{r+1}^n represent the survived features and new augmented features in the $r+1$ -th batch. d_n and n_{r+1} are the dimension of the new augmented features and the number

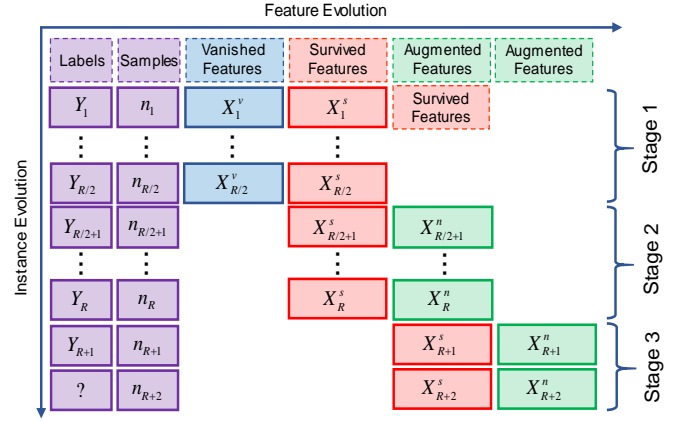


Fig. 3. The illustration of our EML model in multi-shot scenario. When $M = 2$, Stage 1 and Stage 2 share survived features with red color, and Stage 2 and Stage 3 share augmented features with green colors.

of samples. Thus, the goal of this stage is to use $\{X_{r+1}, Y_{r+1}\}$ for training and make the prediction for the $r+2$ -th batch data $X_{r+2} \in \mathbb{R}^{n_{r+2} \times (d_s + d_n)}$ whose number of samples is same as that of $X_{r+1} \in \mathbb{R}^{n_{r+1} \times (d_s + d_n)}$.

To predict the label of the $r+2$ -th batch data, we propose to inherit the metric performance of optimal distance matrix L^s learned on survived features in T-stage, since a set of common survived features exist in both T-stage and I-stage. Although we can construct the triplets directly from the $r+1$ -th batch for training, this simple strategy has two shortcomings: 1) the trained metric model is difficult to be extended into multi-shot scenario; 2) the metric model learned only with the $r+1$ -th batch data will have the worse performance due to the lack of full usage of data in T-stage.

The stack strategy [31], [32] is employed to better inherit the metric performance learned in T-stage. Concretely, let $Z_{r+1}^s = X_{r+1}^s (L^s)^T \in \mathbb{R}^{n_{r+1} \times k}$ as the transformed discriminative metric space, which can be regarded as a new representation of X_{r+1}^s for stacking. X_{r+1} can then be represented as $Z_{r+1} = [Z_{r+1}^s, X_{r+1}^n] \in \mathbb{R}^{n_{r+1} \times (k + d_n)}$. Likewise, X_{r+2} is characterized as Z_{r+2} . We can learn an optimal distance matrix $L^z \in \mathbb{R}^{k \times (k + d_n)}$ on Z_{r+1} with online constructed triplet $(P_{r+1}^z, Q_{r+1}^z, K_{r+1}^z)$, and test the performance on Z_{r+2} , where the samples of P_{r+1}^z and Q_{r+1}^z belong to same class while the samples of P_{r+1}^z and K_{r+1}^z belong to different classes. Formally, at the t -th iterative step, the objective function of learning $L^z \in \mathbb{R}^{k \times (k + d_n)}$ in I-stage can be formulated as:

$$\min_{L^z, F} \frac{1}{2} \|L^z - L_{t-1}^z\|_F^2 + \lambda \text{rank}(L^z) + \frac{\gamma}{2} [W_\sigma(P_{r+1}^z, Q_{r+1}^z) - W_\sigma(P_{r+1}^z, K_{r+1}^z) + 1]_+, \quad (6)$$

where $\gamma \geq 0$ and $\lambda \geq 0$ are the balance parameters. In our experiments, λ and γ are set as the same value in both Eq. (4) and Eq. (6) for simplification. $\text{rank}(L^z)$ denotes the regularization term, which aims to explore the intrinsic low-rank structure of heterogeneous samples in I-stage.

3) *Multi-shot Scenario:* This subsection extends our model into multi-shot scenario. Suppose that there are M stages for

training, *i.e.*, multiple alternating T-stages and I-stages. The m -th stage contains r_m batches, where the features also contain two parts, *i.e.*, survived features and augmented features. Notice that the augmented feature in m -th stage is the survived features in $m + 1$ -th stage. $R = \sum_{m=1}^M r_m$ is denoted as the total number of training batches. The illustration example of multi-shot scenario when $M = 2$ is depicted in Fig. 3. Generally, we have two tasks in the multi-shot scenario, *i.e.*, **1) Task I:** Similarly to the task in one-shot case, we aim to classify testing data X_{R+2} in $M + 1$ -th stage with training data $\{X_{R+1}, Y_{R+1}\}$ and other R batches data of M stages; **2) Task II:** Different from the one-shot scenario, we attempt to make predictions in any batch of any training stage.

IV. MODEL OPTIMIZATION

This section presents an alternating optimization strategy to update our EML model amongst two stages, *i.e.*, T-stage and I-stage, followed by the computational complexity analysis of our model. The whole optimization procedure of our proposed EML model is summarized in **Algorithm 1**.

Note that the low-rank minimization in Eq. (4) and Eq. (6) is a well-known NP hard problem. Take L^z as an example, $\text{rank}(L^z)$ in Eq. (6) can be efficiently surrogated by trace norm $\|L^z\|_*$. Different from traditional Singular Value Thresholding (SVT) [33], we develop a regularization term to guarantee the low-rank property, *i.e.*, $\|L^z\|_* = \text{tr}((L^z L^z)^\top)^{1/2} = \text{tr}(L^z L^z)^\top)^{-1/2} L^z$. As a result, $\text{rank}(L^z)$ in Eq. (6) can be formulated as $\text{tr}(L^z L^z)^\top)^{-1/2} L^z$, where $H^z = (L^z L^z)^\top)^{-1/2}$. Similarly, low rank optimization of L^a and L^s shares same strategy with L^z . $\text{rank}(L^a)$ and $\text{rank}(L^s)$ can be respectively surrogated by $\text{tr}(L^a H^a L^a)^\top)$ and $\text{tr}(L^s H^s L^s)^\top)$, where $H^a = (L^a L^a)^\top)^{-1/2}$ and $H^s = (L^s L^s)^\top)^{-1/2}$.

A. Optimizing T-stage via an Alternating Strategy

1) *Updating L^a by fixing $\{L^s, H^a, F\}$:* With the fixed L^s, H^a and F , the optimization problem in Eq. (4) for solving variable L^a can be concretely expressed as:

$$\begin{aligned} L_t^a = \arg \min_{L^a} & \frac{1}{2} \|L^a - L_{t-1}^a\|_F^2 + \lambda \text{tr}(L^a H^a L^a)^\top) \\ & + \frac{\gamma}{2} [\text{tr}(D(P_i^a, Q_i^a)F) - \text{tr}(D(P_i^a, K_i^a)F) + 1]_+ \\ & + \frac{\rho}{2} [\text{tr}(D(P_i^a, Q_i^s)F) - \text{tr}(D(P_i^a, K_i^s)F) + 1]_+ \\ & + \frac{\rho}{2} [\text{tr}(D(P_i^s, Q_i^a)F) - \text{tr}(D(P_i^s, K_i^a)F) + 1]_+. \end{aligned} \quad (7)$$

The optimal solution of L_t^a can be relaxedly achieved by nulling the gradient of Eq. (7):

$$L_t^a = (L_{t-1}^a - \rho L_t^s (G_3 + G_4)) (I + \lambda H^a + \gamma G_1 + \rho G_2)^{-1}, \quad (8)$$

where $G_1 = Q_i^a \text{diag}(\mathbf{1}^\top F) Q_i^a - K_i^a \text{diag}(\mathbf{1}^\top F) K_i^a - P_i^a \text{diag}(F \mathbf{1}) P_i^a - Q_i^a \text{diag}(F \mathbf{1}) P_i^a + P_i^a \text{diag}(F \mathbf{1}) K_i^a + K_i^a \text{diag}(F \mathbf{1}) P_i^a$, $G_2 = P_i^a \text{diag}(F \mathbf{1}) P_i^a - K_i^a \text{diag}(\mathbf{1}^\top F) K_i^a$, $G_3 = K_i^s \text{diag}(F \mathbf{1}) P_i^a - Q_i^s \text{diag}(F \mathbf{1}) P_i^a + P_i^s \text{diag}(F \mathbf{1}) K_i^s - K_i^s \text{diag}(\mathbf{1}^\top F) K_i^s$, $G_4 = P_i^s \text{diag}(F \mathbf{1}) P_i^s - K_i^s \text{diag}(\mathbf{1}^\top F) K_i^s$.

Algorithm 1 The Optimization of Our Proposed EML Model

Input: The data $\{X_i, Y_i\}_{i=1}^{r+1}$, the parameters γ, λ, ρ ;

Output: L^s and L^z ;

```

1: Initialize:  $L^s, L^a, L^z, F$ ;
2: Transforming Stage (T-stage):
3: for  $i = 1, \dots, r$  do
4:   For data  $X_i$ , calculate the smoothed Wasserstein distance, and construct the triplets for training;
5:   repeat
6:     Fix  $L^a$  and  $L^s$ , solve for distance flow-network  $F$ ;
7:     Update  $L^a$  via Eq. (8);
8:     Update  $L^s$  via Eq. (10);
9:     Update  $H^a$  and  $H^s$  via  $H^a = (L^a L^a)^\top)^{-1/2}$  and  $H^s = (L^s L^s)^\top)^{-1/2}$ ;
10:   until Converge
11: end for
12: Inheriting Stage (I-stage):
13: Represent  $X_{r+1}$  as  $Z_{r+1}$  to calculate smoothed Wasserstein distance, and construct the training triplets;
14: repeat
15:   Fix  $L^z$ , solve for the distance flow-network  $F$ ;
16:   Update  $L^z$  via Eq. (12);
17:   Update  $H^z$  via  $H^z = (L^z L^z)^\top)^{-1/2}$ ;
18: until Converge

```

2) *Updating L^s by fixing $\{L^a, H^s, F\}$:* With the obtained distance matrix L^a and flow matrix F , the optimization problem for variable L^s in Eq. (4) can be denoted as:

$$\begin{aligned} L_t^s = \arg \min_{L^s} & \frac{1}{2} \|L^s - L_{t-1}^s\|_F^2 + \lambda \text{tr}(L^s H^s L^s)^\top) \\ & + \frac{\gamma}{2} [\text{tr}(D(P_i^s, Q_i^s)F) - \text{tr}(D(P_i^s, K_i^s)F) + 1]_+ \\ & + \frac{\rho}{2} [\text{tr}(D(P_i^a, Q_i^s)F) - \text{tr}(D(P_i^a, K_i^s)F) + 1]_+ \\ & + \frac{\rho}{2} [\text{tr}(D(P_i^s, Q_i^a)F) - \text{tr}(D(P_i^s, K_i^a)F) + 1]_+. \end{aligned} \quad (9)$$

Similarly, the updating operator for L_t^s can be given as:

$$L_t^s = (L_{t-1}^s - \rho L_t^a (G_5 + G_8)) (I + \lambda H^s + \gamma G_5 + \rho G_7)^{-1}, \quad (10)$$

where $G_5 = Q_i^s \text{diag}(\mathbf{1}^\top F) Q_i^s - K_i^s \text{diag}(\mathbf{1}^\top F) K_i^s + P_i^s \text{diag}(F \mathbf{1}) P_i^s - P_i^s \text{diag}(F \mathbf{1}) Q_i^s - Q_i^s \text{diag}(F \mathbf{1}) P_i^s$, $G_6 = P_i^a \text{diag}(F \mathbf{1}) P_i^a - P_i^a \text{diag}(F \mathbf{1}) Q_i^s$, $G_7 = Q_i^s \text{diag}(F \mathbf{1}) Q_i^s - K_i^s \text{diag}(\mathbf{1}^\top F) K_i^s$, $G_8 = K_i^a \text{diag}(F \mathbf{1}) P_i^s - Q_i^a \text{diag}(F \mathbf{1}) P_i^s$.

3) *Updating F by fixing $\{L^a, L^s\}$:* When the distance matrices L^a and L^s are fixed, Eq. (4) can be split into some independent traditional smoothed Wasserstein distance subproblems, which can be solved by the method [30]. We omit the detailed process of solving smoothed Wasserstein distance subproblems for simplicity.

B. Optimizing I-stage via an Alternating Strategy

1) *Updating L^z by fixing $\{H^z, F\}$* : Given the fixed H^z and F , the formulation for L^z in Eq. (6) can be rewritten as:

$$L_t^z = \arg \min_{L^z} \frac{1}{2} \|L^z - L_{t-1}^z\|_F^2 + \lambda \text{tr}(L^z H^z L^{z\top}) + \frac{\gamma}{2} [\text{tr}(D(P_{r+1}^z, Q_{r+1}^z)F) - \text{tr}(D(P_{r+1}^z, K_{r+1}^z)F) + 1]_+. \quad (11)$$

By nulling the gradient of Eq. (11), the optimal solution of Eq. (11) for L^z can be given as:

$$L_t^z = L_{t-1}^z (I + \lambda H^z + \gamma G_9)^{-1}, \quad (12)$$

where $G_9 = Q_{r+1}^{z\top} \text{diag}(\mathbf{1}^\top F) Q_{r+1}^z + P_{r+1}^{z\top} F K_{r+1}^z - K_{r+1}^{z\top} \text{diag}(\mathbf{1}^\top F) K_{r+1}^z + K_{r+1}^{z\top} F^\top P_{r+1}^z - P_{r+1}^{z\top} F Q_{r+1}^z - Q_{r+1}^{z\top} F^\top P_{r+1}^z$.

2) *Updating F by fixing L^z* : The optimization procedure of variable F in I-stage is same as that in T-stage: with the fixed L^z , we split the formulation Eq. (6) into some independent traditional smoothed Wasserstein distance subproblem, and solve the variable F via [30].

C. Computational Complexity Analysis

The main computational cost in our EML model involves the updating operations in both T-stage and I-stage. Specifically, in the T-stage, the computational costs of updating L^s and L^a are $O(kd_s + k(d_v + d_s)^2 d_s + d_s^3)$ and $O(k(d_s + d_v) + kd_s^2(d_v + d_s) + (d_v + d_s)^3)$, respectively. For the I-stage, solving the variable L^z in Eq. (6) takes $O((k + d_a)^3)$. Besides, the computational cost of solving F in both T-stage and I-stage is $O(n_p^2 n_q^2 + n_p^2 n_k^2 + n_q^2 n_k^2)$, where $n_p, n_q, n_k \ll n_i$. Since k is usually small when comparing with the number of features and samples, our proposed model is thus computationally efficient in an online manner.

V. EXPERIMENTS

This section first introduces detailed experimental configurations and competing methods. Then the experimental results along with some analyses about our EML model in both one-shot and multi-shot scenarios are provided.

A. Configurations and Competing Methods

The experimental configurations of our EML model in one-shot scenario and some competing methods are detailedly introduced in this subsection.

1) *Experimental Configurations*: As shown in Table I, we conduct extensive comparisons on one real world human motion recognition dataset [13] (*i.e.*, EV-Action) and five synthetic benchmark datasets¹ containing: three digit datasets (*i.e.*, Mnist, Gisette and USPS), one DNA dataset (*i.e.*, Splice) and one image dataset (*i.e.*, Satimage). Specifically, EV-Action dataset [13] is a large-scale human action dataset with 5300 samples, which are collected from three sensors, *i.e.*, depth camera, RGB camera, and skeleton sensors. EV-Action consists of 20 common action classes, where 10 actions are finished

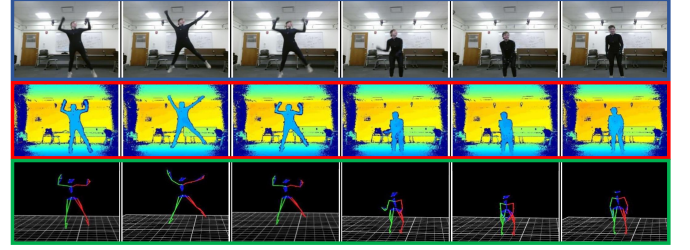


Fig. 4. The examples of human motions in EV-Action dataset, where the first, second and third rows denote the samples collected from depth camera, RGB camera and kinect sensor, respectively.

TABLE I
THE EXPERIMENTAL SETTINGS IN ONE-SHOT SCENARIO.

Datasets	c	$\sum_{i=1}^r n_i$	n_i	d_v	d_s	d_n
EV-Action	20	4200	500, 600, 700	1024	1024	75
Mnist0vs5	2	3200	80, 160, 320	114	228	113
Mnist0vs3vs5	3	4800	120, 240, 480	123	245	121
Splice	2	2240	80, 160, 320	10	40	10
Gisette	2	6000	100, 200, 300	1239	2478	1238
USPS0vs5	2	960	120, 160, 240	64	128	64
USPS0vs3vs5	3	1440	180, 240, 300	64	128	64
Satimage	3	1080	60, 90, 120	10	18	8

by single subject and the others are accomplished by the same subjects interacting with other objects. This dataset is a typical application for features evolution in the real world, where the features collected from depth camera, RGB camera, and skeleton sensors are respectively regarded as vanished, survived and augmented features. Some samples about human actions are visualized as Fig. 4.

For a fair comparison with [21], we adopt the same experimental settings with [21] in both one-shot and multi-shot scenarios, which are elaborated as follows: **1)** The number of samples in each batch is same, *i.e.*, $n_i = n_{r+1} = n_{r+2}$ ($i = [1, 2, \dots, r]$), and the number of samples in each class is equal for all training and test batches; **2)** In T-stage, the total number of training samples is fixed and the number of samples in each batch is varied. Companied with this, the number of training and test samples also changes in the last testing phase; **3)** We assign the first d_v features as vanished features, the next d_s features as survived features and the rest as new augmented features. The first quarter and the last quarter are corresponding vanished and augmented features in our experiments. **4)** All the experimental results are averaged over fifty random repetitions.

2) *Competing Methods*: We validate the superiority of our model by comparing it with: One-pass **Pegasos** [34] assumes that all vanished features are known in I-stage and all augmented features are known in T-stage; **OPMV** [35] regards the vanished and survived features as the first view, the survived and augmented features as the second view; **TCA** [36] assumes the data samples in the T-stage and I-stage come from the source and target domain; **BDML** [2] and **OPML** [7] are the metric learning methods, which only utilize the samples with the augmented features, and ignore the previous vanished features; **OPID** and **OPIDe** [21] propose an one-pass incremental and decremental model for feature evolution.

¹<http://archive.ics.uci.edu/ml/>

TABLE II

COMPARISONS BETWEEN OUR MODEL AND STATE-OF-THE-ART METHODS IN TERMS OF ACCURACY (%) ON SEVEN DATASETS: MEAN AND STANDARD ERRORS AVERAGED OVER FIFTY RANDOM RUNS IN ONE-SHOT SCENARIO. MODELS WITH THE BEST PERFORMANCE ARE BOLDED.

Dataset	n_i	Pegasos [34]	OPMV [35]	TCA [36]	BDML [2]	OPML [7]	OPIDe [21]	OPID [21]	Ours
EV-Action	500	57.38 \pm 1.51	56.37 \pm 1.91	53.88 \pm 2.04	56.42 \pm 0.71	54.10 \pm 1.71	57.84 \pm 1.06	57.57 \pm 1.08	58.87\pm0.68
	600	57.46 \pm 1.60	56.94 \pm 1.82	54.61 \pm 1.73	56.81 \pm 0.65	55.37 \pm 1.64	57.22 \pm 0.95	56.71 \pm 1.40	58.65\pm0.84
	700	57.22 \pm 1.34	56.68 \pm 1.87	54.37 \pm 1.69	56.63 \pm 0.77	55.82 \pm 1.62	57.09 \pm 1.13	56.85 \pm 1.27	58.32\pm0.82
Mnist Ovs5	80	97.74 \pm 0.73	97.39 \pm 0.92	96.53 \pm 1.75	97.00 \pm 1.66	96.45 \pm 1.72	98.68 \pm 0.88	98.88 \pm 0.99	99.85\pm0.91
	160	98.11 \pm 1.03	95.82 \pm 1.84	93.08 \pm 2.94	98.25 \pm 0.80	96.83 \pm 1.38	97.94 \pm 0.97	98.75 \pm 0.90	99.78\pm0.57
	320	97.68 \pm 0.79	96.47 \pm 1.79	92.43 \pm 3.82	98.24 \pm 0.75	96.98 \pm 1.03	97.38 \pm 0.58	97.21 \pm 0.66	99.27\pm0.37
Mnist Ovs3vs5	120	91.47 \pm 3.92	95.87 \pm 1.82	91.26 \pm 3.87	92.23 \pm 2.86	92.42 \pm 2.22	94.58 \pm 1.78	94.97 \pm 1.30	96.91\pm1.38
	240	89.95 \pm 3.08	93.96 \pm 1.18	90.85 \pm 1.74	92.87 \pm 1.40	91.99 \pm 1.64	93.45 \pm 1.41	93.48 \pm 1.35	95.37\pm0.92
	480	90.12 \pm 1.93	93.28 \pm 1.69	91.14 \pm 3.95	93.21 \pm 1.06	92.74 \pm 1.17	93.30 \pm 0.86	93.37 \pm 0.79	95.54\pm0.87
Splice	80	79.65 \pm 4.13	80.13 \pm 3.86	76.93 \pm 4.52	65.65 \pm 5.53	69.60 \pm 4.38	81.22 \pm 3.73	80.50 \pm 3.53	82.65\pm3.32
	160	82.25 \pm 3.26	81.95 \pm 2.84	80.93 \pm 3.47	71.55 \pm 4.07	78.21 \pm 2.53	84.00 \pm 2.03	83.91 \pm 2.05	85.25\pm2.06
	320	82.32 \pm 3.18	78.72 \pm 4.37	81.53 \pm 3.38	72.16 \pm 3.40	80.86 \pm 2.01	85.55 \pm 1.32	85.94 \pm 1.38	87.03\pm1.52
Gisette	100	97.53 \pm 1.33	95.27 \pm 2.85	94.11 \pm 3.35	90.25 \pm 3.13	94.17 \pm 3.02	97.14 \pm 1.28	97.56\pm1.26	97.29 \pm 1.25
	200	95.14 \pm 2.97	94.05 \pm 3.36	93.03 \pm 3.16	91.50 \pm 1.25	93.61 \pm 3.19	95.59 \pm 0.95	95.39 \pm 1.06	96.82\pm0.91
	300	96.84 \pm 1.35	93.71 \pm 3.11	94.37 \pm 3.72	93.83 \pm 2.12	93.77 \pm 2.96	96.36 \pm 0.69	95.33 \pm 0.93	97.89\pm0.43
USPS Ovs5	120	98.52\pm0.67	95.27 \pm 2.67	96.42 \pm 1.81	95.90 \pm 1.65	93.72 \pm 2.32	96.17 \pm 1.44	96.51 \pm 1.25	97.23 \pm 1.64
	160	97.84 \pm 0.82	95.65 \pm 1.72	95.46 \pm 2.13	96.38 \pm 1.23	93.04 \pm 4.05	96.78 \pm 1.31	96.93 \pm 1.00	98.91\pm0.67
	240	97.93 \pm 0.72	96.17 \pm 1.28	95.85 \pm 2.07	96.78 \pm 1.18	93.62 \pm 3.01	94.93 \pm 1.28	95.06 \pm 1.10	98.94\pm0.70
USPS Ovs3vs5	180	94.68 \pm 1.20	92.46 \pm 1.07	93.88 \pm 1.37	90.62 \pm 2.48	92.06 \pm 1.64	94.47 \pm 1.77	94.13 \pm 1.92	95.73\pm0.88
	240	94.39 \pm 1.09	91.69 \pm 2.31	92.94 \pm 1.58	91.48 \pm 1.68	91.23 \pm 1.73	92.08 \pm 1.93	92.50 \pm 1.66	95.52\pm1.26
	300	95.47\pm0.94	92.25 \pm 1.60	93.26 \pm 1.44	92.13 \pm 1.09	91.60 \pm 1.71	92.95 \pm 1.12	92.67 \pm 1.46	94.05 \pm 1.46
Satimage	60	94.25 \pm 2.56	96.48 \pm 1.47	97.25 \pm 1.08	97.14 \pm 1.59	97.47 \pm 1.59	98.17 \pm 2.19	97.60 \pm 2.31	99.20\pm0.91
	90	96.49 \pm 1.49	96.83 \pm 1.18	96.52 \pm 1.32	97.62 \pm 1.52	97.69 \pm 1.16	98.58 \pm 1.12	97.29 \pm 2.08	99.71\pm1.06
	120	98.03 \pm 1.13	97.38 \pm 1.94	97.12 \pm 1.87	97.12 \pm 1.48	97.15 \pm 1.49	98.45 \pm 1.14	96.85 \pm 1.94	99.52\pm1.07

TABLE III

ABLATION STUDY OF OUR EML MODEL IN ONE-SHOT SCENARIO.

Dataset	n_i	Ours-woT	Ours-woI	Ours-woW	Ours
EV-Action	500	56.68 \pm 1.74	54.36 \pm 1.61	57.93 \pm 0.85	58.33\pm0.76
	600	56.23 \pm 1.81	55.70 \pm 1.49	57.70 \pm 1.04	57.94\pm0.88
	700	57.02 \pm 1.56	55.93 \pm 1.76	57.83 \pm 0.92	58.12\pm0.86
Mnist Ovs5	80	97.85 \pm 1.24	96.70 \pm 1.71	98.90 \pm 0.97	99.07\pm0.94
	160	97.54 \pm 1.46	96.84 \pm 1.85	98.87 \pm 1.06	99.22\pm0.61
	320	97.23 \pm 3.34	96.88 \pm 0.96	98.95 \pm 0.83	99.27\pm0.37
Mnist Ovs3vs5	120	94.55 \pm 1.48	92.78 \pm 2.11	96.02 \pm 1.85	96.53\pm1.49
	240	93.49 \pm 1.07	92.88 \pm 1.31	94.88 \pm 1.37	95.37\pm0.92
	480	94.32 \pm 0.81	93.37 \pm 1.13	95.13 \pm 1.22	95.54\pm0.87
Splice	80	81.58 \pm 3.10	70.83 \pm 4.47	82.45 \pm 3.38	82.65\pm3.32
	160	84.07 \pm 2.51	78.87 \pm 3.01	84.87 \pm 2.19	85.25\pm2.06
	320	84.85 \pm 2.38	81.56 \pm 1.99	85.94 \pm 1.61	86.40\pm1.59
Gisette	100	95.22 \pm 1.30	92.47 \pm 1.68	96.84 \pm 1.40	97.29\pm1.25
	200	94.38 \pm 1.52	92.96 \pm 1.75	96.27 \pm 1.53	96.82\pm0.91
	300	96.11 \pm 0.95	95.08 \pm 1.19	97.14 \pm 0.87	97.79\pm0.46
USPS Ovs5	120	95.42 \pm 1.82	94.82 \pm 2.02	96.26 \pm 1.33	97.23\pm1.64
	160	96.04 \pm 1.33	94.95 \pm 1.70	97.03 \pm 1.47	98.31\pm0.82
	240	96.35 \pm 1.06	95.17 \pm 1.16	97.24 \pm 0.96	98.87\pm0.74
USPS Ovs3vs5	180	93.36 \pm 1.77	91.97 \pm 2.00	94.86 \pm 1.17	95.28\pm0.96
	240	93.13 \pm 1.38	92.01 \pm 1.45	94.33 \pm 1.54	94.96\pm1.37
	300	92.99 \pm 1.35	91.81 \pm 1.67	93.47 \pm 1.83	94.05\pm1.46
Satimage	60	96.50 \pm 1.59	97.43 \pm 1.36	98.31 \pm 1.10	98.97\pm0.95
	90	96.78 \pm 2.72	97.31 \pm 1.10	98.19 \pm 1.16	98.71\pm1.13
	120	96.22 \pm 1.91	97.23 \pm 1.22	98.02 \pm 1.22	98.53\pm1.20

B. Experiments in One-shot Scenario

In this subsection, we present the comprehensive experimental analysis, ablation studies, effects of hyper-parameters and convergence investigations of our EML model in one-shot scenario, followed by computational costs of model optimization.

1) *Experimental Analysis*: The experimental results for one-shot scenario are shown in Table II. From the presented results, we have the following observations: **1)** Although our model cannot access the vanished features in T-stage and the augmented features in I-stage, both transforming and inheriting strategies can efficiently exploit useful information of vanished feature and expand it into augmented features. **2)** Our model can be successfully applied into both high-dimensional (e.g., EV-Action and Gisette) and low-dimensional (e.g., Satimage) feature evolution, which are the challenging tasks to explore

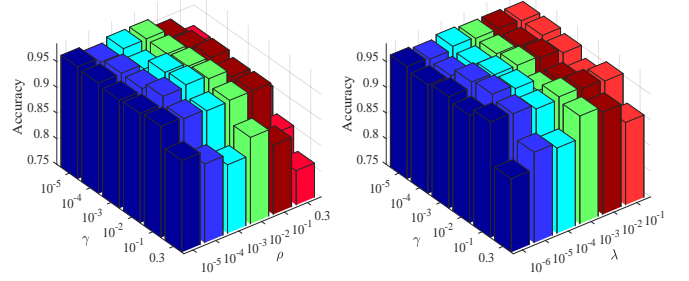


Fig. 5. Effects of parameters $\{\gamma, \rho\}$ when $\lambda = 10^{-4}$ (left), and $\{\gamma, \lambda\}$ when $\rho = 10^{-3}$ (right) on the USPS0vs5 dataset.

the data structure with the existing features; **3)** When we use the learned distance matrix in T-stage to assist training in I-stage, the testing performance of our model increases significantly, even though the training samples in I-stage are relatively rare, i.e., n_i contains a small number of samples in I-stage. **4)** Our model performs better than OPID and OPIDe [21], since T-stage could explore important information from vanished features, and I-stage efficiently inherits the metric performance from T-stage to take advantage of augmented features.

2) *Ablation Studies*: To validate the effectiveness of our model, we intend to study the effects of different components of our model, i.e., training without T-stage (denoted as Ours-woT), training without I-stage (denoted as Ours-woI) and training without the Wasserstein distance metric (denoted as Ours-woW). From the presented results in Table. III, notice that our model has the best performance when both transforming and inheriting strategies work together to tackle incremental and decremental features via the Wasserstein distance metric, which validates the reasonable design of our model. Compared with other metric distances (e.g., Mahalanobis distance), the smoothed Wasserstein distance could

TABLE IV

COMPUTATIONAL TIME IN TERMS OF MINUTES: MEAN AND STANDARD ERRORS AVERAGED OVER FIFTY RANDOM RUNS IN ONE-SHOT SCENARIO.

	Pegasos [34]	OPMV [35]	TCA [36]	BDML [2]	OPML [7]	OPIDe [21]	OPID [21]	Ours
EV-Action ($n_i = 500$)	27.11 \pm 0.04	28.58 \pm 0.04	37.72 \pm 0.09	36.18 \pm 0.18	22.95\pm0.07	26.47 \pm 0.09	26.33 \pm 0.14	25.48 \pm 0.06
Mnist0vs5 ($n_i = 80$)	6.18 \pm 0.07	7.45 \pm 0.06	14.96 \pm 0.12	16.27 \pm 0.10	3.84\pm0.04	5.13 \pm 0.11	4.95 \pm 0.07	4.68 \pm 0.05
USPS0vs5 ($n_i = 120$)	3.16 \pm 0.02	4.75 \pm 0.10	11.93 \pm 0.04	13.06 \pm 0.12	1.24\pm0.03	1.93 \pm 0.05	1.87 \pm 0.06	1.53 \pm 0.08
Gisette ($n_i = 100$)	40.52 \pm 0.03	41.06 \pm 0.16	51.28 \pm 0.04	49.73 \pm 0.14	35.26\pm0.03	38.24 \pm 0.08	39.15 \pm 0.05	37.57 \pm 0.11
Satimage ($n_i = 120$)	2.64 \pm 0.05	3.08 \pm 0.10	10.23 \pm 0.07	11.47 \pm 0.09	0.52\pm0.02	0.66 \pm 0.04	0.71 \pm 0.08	0.68 \pm 0.03

TABLE V

COMPARISONS BETWEEN OUR MODEL AND STATE-OF-THE-ART METHODS IN TERMS OF ACCURACY (%) ON FOUR DATASETS: MEAN AND STANDARD ERRORS AVERAGED OVER FIFTY RANDOM RUNS IN MULTI-SHOT SCENARIO FOR TASK I. MODELS WITH THE BEST PERFORMANCE ARE BOLD.

Dataset	n_i	Pegasos [34]	OPMV [35]	TCA [36]	BDML [2]	OPML [7]	OPIDe [21]	OPID [21]	Ours
Mnist	80	97.50 \pm 1.82	88.75 \pm 4.99	93.14 \pm 1.87	92.25 \pm 2.20	93.92 \pm 3.22	95.70 \pm 2.17	95.92 \pm 2.23	98.54\pm1.08
	160	97.56 \pm 1.28	90.75 \pm 3.02	91.78 \pm 2.43	95.70 \pm 1.26	94.34 \pm 1.54	95.53 \pm 1.61	95.29 \pm 1.80	98.61\pm0.57
	320	97.61 \pm 0.90	92.72 \pm 1.76	90.35 \pm 2.67	96.06 \pm 0.98	95.20 \pm 0.96	95.22 \pm 1.33	95.04 \pm 1.39	98.73\pm0.64
Gisette	100	91.58 \pm 2.87	86.24 \pm 4.76	91.28 \pm 2.56	90.48 \pm 3.29	89.87 \pm 3.62	95.08 \pm 2.35	94.36 \pm 1.88	96.12\pm1.18
	200	90.68 \pm 1.79	88.41 \pm 3.00	90.92 \pm 2.84	90.69 \pm 2.73	92.22 \pm 2.03	94.88 \pm 1.39	93.81 \pm 1.50	95.94\pm1.72
	300	91.18 \pm 1.13	89.42 \pm 2.27	92.13 \pm 2.14	92.52 \pm 1.71	91.83 \pm 1.61	94.65 \pm 1.12	93.91 \pm 1.45	95.71\pm1.68
USPS	120	97.48 \pm 0.12	94.95 \pm 2.46	92.87 \pm 2.16	96.08 \pm 1.36	93.83 \pm 2.13	94.77 \pm 1.62	94.61 \pm 1.69	98.57\pm0.94
	160	97.56 \pm 0.19	95.17 \pm 2.18	93.05 \pm 1.94	96.24 \pm 1.55	94.21 \pm 1.66	94.13 \pm 1.54	94.51 \pm 1.30	98.68\pm0.65
	240	97.37 \pm 0.41	95.58 \pm 1.06	92.72 \pm 2.33	97.57 \pm 0.67	94.62 \pm 1.25	93.92 \pm 1.47	93.62 \pm 1.16	98.39\pm0.72
USPS	180	92.03 \pm 1.57	89.22 \pm 3.21	90.86 \pm 2.87	90.91 \pm 1.81	88.61 \pm 2.84	84.05 \pm 2.27	83.34 \pm 2.36	93.11\pm1.87
	240	90.90 \pm 1.40	89.13 \pm 2.05	90.24 \pm 2.93	91.98 \pm 2.04	89.62 \pm 2.17	84.68 \pm 1.73	84.49 \pm 1.92	93.23\pm1.58
	300	90.48 \pm 1.24	89.52 \pm 1.59	89.85 \pm 3.16	92.61 \pm 1.23	89.46 \pm 1.80	83.25 \pm 1.61	83.17 \pm 1.66	93.13\pm1.55

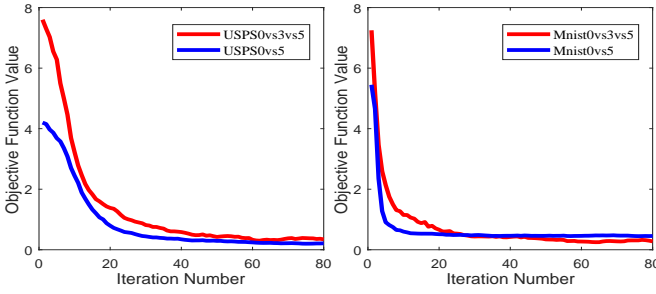


Fig. 6. The convergence analysis of our model on the USPS (left) and Mnist (right) dataset in one-shot scenario.

better characterize the similarity relations among the complex and heterogeneous data, since the evolving features in different stages are not strictly aligned. Both T-stage and I-stage play an essential role in tracking instance and feature evolutions simultaneously.

3) *Effects of Hyper-Parameters*: In this subsection, we conduct the parameter experiments on USPS0vs5 dataset as an example to investigate the effects of parameters γ , λ and ρ . As shown in Fig. 5, we present the experimental results averaged over fifty random repetitions by tuning γ , ρ in range of $\{10^{-5}, 10^{-4}, 10^{-3}, 10^{-2}, 10^{-1}, 0.3\}$ and λ in range of $\{10^{-6}, 10^{-5}, 10^{-4}, 10^{-3}, 10^{-2}, 10^{-1}\}$. Notice that our model achieves the best performance when $\gamma = 10^{-2}$, $\rho = 10^{-3}$ and $\lambda = 10^{-4}$. Moreover, our model has greatly stable performance over the wide range of different parameters.

4) *Convergence Investigations*: The convergence condition of **Algorithm 1** is depending on the little change (we set it as 2.5×10^{-5}) in the consecutive objective function values, and Fig. 6 depicts the convergence curves of our EML model on Mnist and USPS datasets. From the presented results in Fig. 6, we can notice that our model can converge asymptotically to a

stable value with respect to the objective function value after a few iterations. Furthermore, It validates that our proposed optimization algorithm could efficiently achieve stable performance with appropriate convergence condition.

5) *Computational Costs*: Table IV presents the computational costs (i.e., optimization time) of our proposed EML model and other competing methods. From the reported results, we can conclude that: 1) Our model is computationally efficient in an online manner for large-scale applications since $n_p, n_q, n_k \ll n_i$ and k is usually a small value when compared with the number of feature dimension and samples. 2) The computational time costs (by the minute) of our model are less than other competing methods about 0.67~13.71 minutes on most experimental datasets except for OPML [7], since OPML only takes advantage of training samples in I-stage for model optimization procedure.

C. Experiments in Multi-shot Scenario

This subsection introduces the experimental configurations and comparison performance of our EML model in multi-shot scenario.

1) *Experimental Configurations*: In multi-shot scenario, we take $M = 2$, i.e., two-shot scenario with three stages for illustration, as shown in Fig. 3. The data used in one-shot scenario is split into three stages. The additional experimental configurations for multi-shot scenario are: **1)** All batches of T-stage in one-shot scenario are split into Stage 1 and Stage 2 with equal number of samples. In this setting, Stage 1 is T-stage, Stage 2 is E-stage, whereas Stage 2 is both I-stage (corresponding to T-stage of Stage 1) and T-stage (corresponding to I-stage of Stage 3). **2)** We split all the features into four equal parts with the original order. Concretely, Stage 1 and Stage 2 share the second part. Stage 2 and Stage 3 share the third part. The first part in Stage 1 is the vanished features and the last part in Stage 3 is the augmented features.

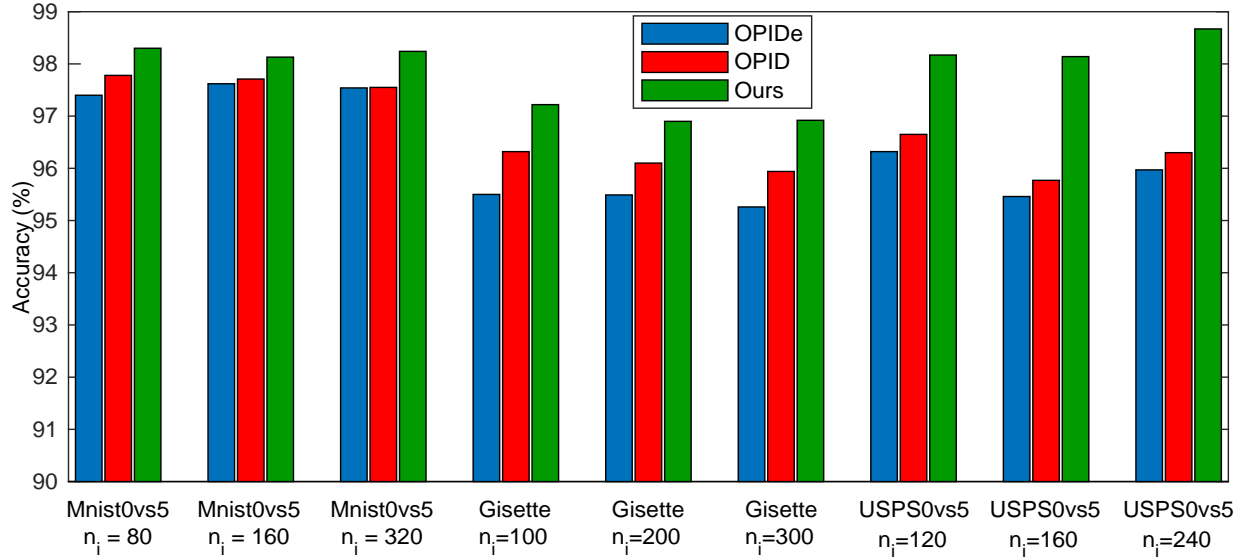


Fig. 7. Comparisons in terms of accuracy (%) on three datasets: mean and standard errors averaged over fifty random runs in multi-shot scenario for Task II.

2) *Experiments for Task I and II*: To address the **Task I**, we directly use the last adjacent two stages and regard it as the one-shot scenario for predictions since the data in the most adjacent stage share common features. Concretely, we can use the transforming strategy shown in Eq. (4) on data in Stage 2 to learn the optimal distance matrix. After that, the inheriting strategy shown in Eq. (6) is applied to make predictions in Stage 3. To tackle the **Task II**, we regard the adjacent two stages as one-shot scenario and repeat this procedure until the last stage. Specially, the previous transforming and inheriting strategies are integrated into the first adjacent stage and predict on the second batch data of Stage 2. After inheriting the metric performance of Stage 1, with new-coming labeled data in Stage 2, we can also extract the useful information in survived features of Stage 2 and forward it into the augmented features via common discriminative space. Then we perform the inheriting strategy on survived features in Stage 3 to assist following predictions.

The experimental results averaged over fifty random repetitions for Task I and II are shown in Table V and Fig. 7. Notice that: 1) Our model can be successfully extended from one-shot case into multi-shot scenario to address Task I and Task II. 2) Compared with Task I, our model performs better for Task II in most cases since the features existing in Stage 1 are also used to assist the predictions at any batches. 3) Our model significantly outperforms OPIDe and OPID especially in Task I since it could inherit the metric performance of survived features in any most adjacent stages.

VI. CONCLUSION

In this paper, we propose an online Evolving Metric Learning (EML) model for both instance and feature evolutions, which is successfully applied into both one-shot and multi-shot scenarios. Our model contains two essential stages, *i.e.*, T-stage and I-stage. To be specific, for the T-stage, we use survived features to represent the important information of both vanished and survived features by exploiting a common

metric space. In the I-stage, we inherit the metric performance of survived features from T-stage and extend it into the augmented features. Experiments on several benchmark datasets verify the superiority of our EML model. In the future, we will consider lifelong learning for both instance and feature evolutions, which learns new streaming evolution tasks without catastrophic forgetting for original evolution tasks.

REFERENCES

- [1] H. V. Nguyen and L. Bai, "Cosine similarity metric learning for face verification," in *Computer Vision – ACCV 2010*, R. Kimmel, R. Klette, and A. Sugimoto, Eds., 2011, pp. 709–720.
- [2] J. Xu, L. Luo, C. Deng, and H. Huang, "Bilevel distance metric learning for robust image recognition," in *Proceedings of the 32Nd International Conference on Neural Information Processing Systems*, 2018, pp. 4202–4211.
- [3] Z. Boukouvalas, "Distance metric learning for medical image registration," 2011.
- [4] G. Chechik, V. Sharma, U. Shalit, and S. Bengio, "Large scale online learning of image similarity through ranking," *J. Mach. Learn. Res.*, vol. 11, pp. 1109–1135, Mar. 2010.
- [5] P. Jain, B. Kulis, I. S. Dhillon, and K. Grauman, "Online metric learning and fast similarity search," in *Advances in Neural Information Processing Systems 21*, 2009, pp. 761–768.
- [6] K. Q. Weinberger and L. K. Saul, "Distance metric learning for large margin nearest neighbor classification," *J. Mach. Learn. Res.*, vol. 10, pp. 207–244, Jun. 2009.
- [7] W. Li, Y. Gao, L. Wang, L. Zhou, J. Huo, and Y. Shi, "Opml: A one-pass closed-form solution for online metric learning," *Pattern Recognition*, vol. 75, pp. 302 – 314, 2018.
- [8] R. Jin, S. Wang, and Y. Zhou, "Regularized distance metric learning: theory and algorithm," in *Advances in Neural Information Processing Systems 22*, 2009, pp. 862–870.
- [9] B. Shaw, B. Huang, and T. Jebara, "Learning a distance metric from a network," in *Advances in Neural Information Processing Systems 24*, 2011, pp. 1899–1907.
- [10] J. V. Davis, B. Kulis, P. Jain, S. Sra, and I. S. Dhillon, "Information-theoretic metric learning," in *Proceedings of the 24th International Conference on Machine Learning*. ACM, 2007, pp. 209–216.
- [11] G. Sun, C. Yang, J. Liu, L. Liu, X. Xu, and H. Yu, "Lifelong metric learning," *IEEE Transactions on Cybernetics*, vol. 49, no. 8, pp. 3168–3179, 2019.
- [12] B. Nguyen, C. Morell, and B. De Baets, "Scalable large-margin distance metric learning using stochastic gradient descent," *IEEE Transactions on Cybernetics*, vol. 50, no. 3, pp. 1072–1083, 2020.

- [13] L. Wang, B. Sun, J. P. Robinson, T. Jing, and Y. Fu, "Ev-action: Electromyography-vision multi-modal action dataset," *arXiv preprint arXiv:1904.12602*, 2019.
- [14] C. K. Ho, A. Robinson, D. R. Miller, and M. J. Davis, "Overview of sensors and needs for environmental monitoring," *Sensors*, vol. 5, no. 1, pp. 4–37, 2005.
- [15] S. Shalev-Shwartz, Y. Singer, and A. Y. Ng, "Online and batch learning of pseudo-metrics," in *Proceedings of the Twenty-first International Conference on Machine Learning*. ACM, 2004, p. 94.
- [16] B. Nguyen and B. De Baets, "Kernel-based distance metric learning for supervised k -means clustering," *IEEE Transactions on Neural Networks and Learning Systems*, vol. 30, no. 10, pp. 3084–3095, Oct 2019.
- [17] Q. Qian, R. Jin, J. Yi, L. Zhang, and S. Zhu, "Efficient distance metric learning by adaptive sampling and mini-batch stochastic gradient descent (sgd)," *Machine Learning*, vol. 99, no. 3, pp. 353–372, Jun 2015.
- [18] X. Gao, S. C. H. Hoi, Y. Zhang, J. Wan, and J. Li, "Soml: Sparse online metric learning with application to image retrieval," in *AAAI*, 2014.
- [19] H. Xia, S. C. H. Hoi, R. Jin, and P. Zhao, "Online multiple kernel similarity learning for visual search," *IEEE Transactions on Pattern Analysis and Machine Intelligence*, vol. 36, no. 3, pp. 536–549, March 2014.
- [20] B.-J. Hou, L. Zhang, and Z.-H. Zhou, "Learning with feature evolvable streams," in *Proceedings of the 31st International Conference on Neural Information Processing Systems*, 2017, pp. 1416–1426.
- [21] C. Hou and Z.-H. Zhou, "One-pass learning with incremental and decremental features," *IEEE Transactions on Pattern Analysis and Machine Intelligence*, vol. 40, pp. 2776–2792, 2018.
- [22] H.-J. Ye, D.-C. Zhan, Y. Jiang, and Z.-H. Zhou, "Rectify heterogeneous models with semantic mapping," in *ICML*, 2018.
- [23] Q. Zhang, P. Zhang, G. Long, W. Ding, C. Zhang, and X. Wu, "Towards mining trapezoidal data streams," *2015 IEEE International Conference on Data Mining*, pp. 1111–1116, 2015.
- [24] Q. Zhang, P. Zhang, G. Long, W. Ding, C. Zhang, and X. Wu, "Online learning from trapezoidal data streams," *IEEE Transactions on Knowledge and Data Engineering*, vol. 28, no. 10, pp. 2709–2723, Oct 2016.
- [25] C. Hu, Y. Chen, X. Peng, H. Yu, C. Gao, and L. Hu, "A novel feature incremental learning method for sensor-based activity recognition," *IEEE Transactions on Knowledge and Data Engineering*, vol. 31, no. 6, pp. 1038–1050, June 2019.
- [26] K. Crammer, O. Dekel, J. Keshet, S. Shalev-Shwartz, and Y. Singer, "Online passive-aggressive algorithms," *J. Mach. Learn. Res.*, vol. 7, pp. 551–585, Dec. 2006.
- [27] J. Xu, L. Luo, C. Deng, and H. Huang, "Multi-level metric learning via smoothed wasserstein distance," in *IJCAI*, 2018, pp. 2919–2925.
- [28] R. Sandler and M. Lindenbaum, "Nonnegative matrix factorization with earth mover's distance metric for image analysis," *IEEE Transactions on Pattern Analysis and Machine Intelligence*, vol. 33, pp. 1590–1602, Aug 2011.
- [29] M. Cuturi, "Sinkhorn distances: Lightspeed computation of optimal transport," in *Proceedings of the 26th International Conference on Neural Information Processing Systems - Volume 2*, 2013, pp. 2292–2300.
- [30] A. Rolet, M. Cuturi, and G. Peyr, "Fast dictionary learning with a smoothed wasserstein loss," in *Proceedings of the 19th International Conference on Artificial Intelligence and Statistics*, vol. 51, 09–11 May 2016, pp. 630–638.
- [31] L. Breiman, "Stacked regressions," *Machine Learning*, vol. 24, pp. 49–64, Jul 1996.
- [32] Z.-H. Zhou, *Ensemble Methods: Foundations and Algorithms*. Chapman & Hall/CRC, 2012.
- [33] J.-F. Cai, E. J. Cands, and Z. Shen, "A singular value thresholding algorithm for matrix completion," *SIAM Journal on Optimization*, vol. 20, no. 4, pp. 1956–1982, 2010.
- [34] S. Shalev-Shwartz, Y. Singer, N. Srebro, and A. Cotter, "Pegasos: primal estimated sub-gradient solver for svm," *Mathematical Programming*, vol. 127, pp. 3–30, Mar 2011.
- [35] Y. Zhu, W. Gao, and Z.-H. Zhou, "One-pass multi-view learning," in *ACML*, 2015.
- [36] S. J. Pan, I. W. Tsang, J. T. Kwok, and Q. Yang, "Domain adaptation via transfer component analysis," *IEEE Transactions on Neural Networks*, vol. 22, no. 2, pp. 199–210, Feb 2011.